Chapter 9

Properties of Clouds and Cloud Systems

William B. Rossow
NASA Goddard Institute for Space Studies
New York, NY 10025
USA

9.1 Introduction

Observations of clouds from the surface, aircraft and spacecraft give the impression of great complexity and variability. Quantitative descriptions of the variety of clouds and determination of its causes have been limited by lack of comprehensive and systematic observations that cover the full range of space and time scales over which clouds vary. Now, there are two cloud datasets that cover scales from 30 km and 3 hr up to the whole globe for more than a decade, giving us, for the first time, a truly global view of clouds and their variability. One dataset provides information on cloud cover, cloud base heights and cloud morphology from several decades of surface weather observations (Warren et al., 1986, 1988; Hahn et al., 1995). These observations can be supplemented by balloon measurements of the profiles of atmospheric temperature and humidity that can provide information about cloud layer structure (Poore et al., 1995; Wang and Rossow, 1995). Much more detailed cloud observations of global cloudiness are possible using satellite remote sensing. A comprehensive survey of cloud cover, cloud top temperature/pressure and visible optical thickness has been produced from more than a decade of observations from the international constellation of weather satellites (Schiffer and Rossow, 1983; Rossow and Schiffer, 1991). Newer satellite instruments and analysis techniques extend the list of cloud properties that can be measured by satellites. Combining all of these results provides the best available survey of cloud properties and also indicates what satellite instruments should be included in a future cloud observing system.

9.2 Remote Sensing of Clouds

Satellites measure radiation, so a physical model of the interaction of radiation in cloudy atmospheres is needed to retrieve cloud properties from the satellite measurements (e.g. Goody

NATO ASI Series, Vol. I 45
Radiation and Water in the Climate System:
Remote Measurements
Edited by Ehrhard Raschke

and Yung, 1989; Stephens, 1994). The type of radiation measured determines the kind of radiative transfer model. The intensity of reflected sunlight (0.30–4.0 μm wavelengths) can be measured, as well as its variation with wavelength or, since the source is uni-directional, the amount and direction of polarization can be determined. The intensity of thermal emission in the infrared (4.0–200 μm wavelengths) or microwave (1 mm–10 cm wavelengths) can be measured as well as its variations with wavelength; microwave polarization is also a useful indication of scattering processes. All of these approaches depend on natural sources of radiation, but satellite instruments can also emit coherent forms of radiation and measure their interaction with clouds: lidars emit radiation in the wavelength ranges of sunlight and infrared and radars emit microwave radiation. These types of radiation are much easier to separate from natural radiation because they are emitted at sharply defined wavelengths and polarizations. Table 9.1 lists various properties of clouds that will be discussed in later sections and remote sensing techniques that have been developed to measure them.

Optical thickness	Intensity of reflected sunlight, Spectrum of emitted IR, Intensity of reflected lidar or radar, Intensity of emitted microwave
Particle size	Spectrum and/or Polarization of reflected sunlight, Spectrum of emitted IR, Spectrum and/or Polarization of scattered microwave
Particle shape	Angular distribution of Intensity and/or Polarization of reflected sunlight or lidar
Particle size variance	Polarization of reflected sunlight
Number density	Derived from optical thickness and particle size
Liquid water path	Derived from optical thickness (and particle size)
Ice water path	Derived from optical thickness (and particle size)
Precipitation	Intensity and/or polarization of emitted microwave, Intensity of reflected radar
Cloud top location	Spectrum and/or Polarization of reflected sunlight, Solar extinction, Intensity and/or spectrum of emitted IR, Timing of returned lidar or radar pulse
Cloud base location	Spectrum of emitted IR, Timing of returned lidar or radar pulse

Table 9.1: *Satellite remote sensing techniques used to determine cloud properties.*

The most extensively used method to measure cloud optical thickness from satellites employs measurements of the intensity of reflected sunlight (Rossow et al., 1989; Rossow and Schiffer, 1991). This method is less sensitive at low optical thicknesses (< 1), but still effective at very large values (> 60). Although the spectrum of emitted IR can be used to determine lower optical thicknesses (< 10) (Carlson et al., 1993), this technique has not been used for Earth observations. A simpler approach uses IR intensities measured from satellites at a few discrete wavelengths to estimate lower optical thicknesses from transmitted thermal emission (Wylie and Menzel, 1989; Wylie et al., 1994). The results from all of these techniques depend on particle size, whereas measurements of thermal emission in the microwave can be used to measure optical thickness (or water path) for liquid water clouds over oceans independently of particle size. Microwave techniques are insensitive to low cloud optical thicknesses (< 7) but are more sensitive at very large values (> 100). Several limited satellite microwave analyses have

been completed (Greenwald et al., 1993; Liu and Curry, 1992, 1993; Lin and Rossow, 1994). Ice crystals in clouds are too small to affect microwave emissions; but combining reflected sunlight (or IR spectra) with microwave can be used to estimate ice water path from satellites (Lin and Rossow, 1994). Lidar and millimeter radar scattering can also be used to estimate ice water path (Sassen et al., 1989; Kropfli, 1995): lidar is most sensitive to very low optical thicknesses (< 0.5), whereas radar remains useful up to very large values (> 60). These techniques are more sensitive to particle sizes, however. Radar has not been used on satellites yet; one lidar has flown on the Shuttle (McCormick et al., 1995).

Cloud particle sizes (dimensions in the range from 6–60 μm) have been determined for liquid water clouds on Earth from satellite measurements of the wavelength dependence of reflected sunlight (Han et al., 1994). IR spectra can also be used, especially for the larger size particles occurring in ice clouds (Carlson et al., 1993), but this has not been done for Earth observations. Size information for precipitation-sized particles (dimensions > 500 μm) can be determined from centimeter radar scattering, but this has not been done from satellites yet (an experimental mission is planned for 1997: the Tropical Rainfall Measuring Mission).

Retrieval of particle sizes is especially sensitive to particle shape when using observations of reflected sunlight; hence, measurements of the angular distribution of reflected intensity and polarization can be used, in principle, to infer particle shape but this technique has not been tried before.

There are many different methods for determining cloud top location from satellite measurements. Two that have not been used for Earth observations but have been used on other planets are measuring the strength of gas absorption features, giving the amount of gas over the cloud, and measuring the amount of Rayleigh scattering from the polarization of reflected sunlight, giving the pressure at cloud top (Travis et al., 1978). Timing the return pulses from lidar and radar gives a more direct estimate of cloud top height, but only the former has recently been attempted from space (LITE mission on Shuttle). Two more extensively used methods are determining heights at which sunlight is extinguished when the Earth's limb occults the sun (Woodbury and McCormick, 1986; Kent et al., 1993; Wang et al., 1995) and determining cloud top temperature from IR emissions (Rossow et al., 1989; Wylie and Menzel, 1989; Wylie et al., 1994).

Cloud base location can sometimes be determined from the spectrum of IR emission, if cloud optical thickness is low enough (Minnis et al., 1995). Also, lidar can determine cloud base if it can penetrate the whole cloud layer (Sassen et al., 1989). Millimeter radar can penetrate much thicker clouds and would provide a more general survey of cloud vertical structure, but such an instrument has never been flown on a satellite.

9.3 Summary of Observed Cloud Properties

Clouds exhibit a very wide range of properties from the thinnest wisps of ice cirrus clouds at 15–20 km altitude or small clumps of liquid cumulus clouds near the surface to the violent storm clouds that extend throughout the whole depth of the troposphere and produce heavy rainfall. Cirrus have very little water content, occupy thin layers, and may have patchy horizontal coverage. Storm cloud systems have nearly the maximum possible water content, occupy multiple or very deep layers, and can cover areas more than 1000 km across. Table 9.2 lists cloud properties in order of decreasing significance in determining microphysical processes in clouds, including precipitation, and in determining radiative transfer in clouds. Figures 9.1–9.4 summarize the distributions of some of these properties obtained from extensive surveys of weather observations and satellite remote sensing.

	Microphysics Rank	Radiation Rank
Cloud cover	1	1
Liquid/Ice water path	2	2
Layer thickness	2	4
Particle size	3	5
Vertical structure	4	4
Particle size variance	5	6
Top/base height/temperature	6	3
Variance of water content	7	5
Particle shape	8	6

Table 9.2: *Cloud properties in order of decreasing significance for microphysical (first number) and radiative transfer (second number) processes.*

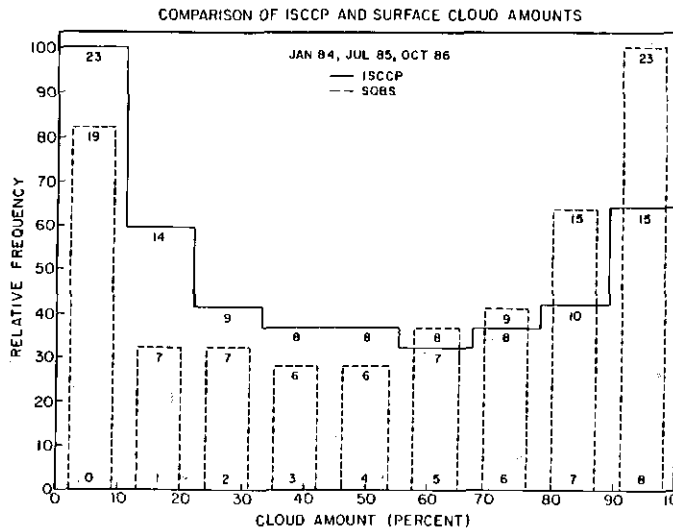

Figure 9.1: *Frequency distributions of cloud amount observed from satellites (solid line) and from the surface (dashed line) (from Rossow et al., 1993).*

Cloud amount, even at the relatively large spatial scale of the satellite results (280 km) is still dominated by either complete absence or complete cover (Rossow et al., 1993), producing a bi-modal distribution in Figure 9.1. Most of the other cloud property distributions have a characteristic shape: most clouds have properties in a relatively narrow range near the most frequent value, but about a quarter to one third of the population has values spread over a very much larger range. Cloud layer thicknesses are concentrated below 1 km, but some clouds have thicknesses greater than 8 km (Figure 9.2). Even the height distributions for two-layer clouds show a concentration of the lower layers in the boundary layer near 1 km height, but the upper layers are spread throughout the troposphere (Figure 9.3). This explains the broad distribution of cloud top pressures (Figure 9.4a); however, the corresponding optical thicknesses

are highly concentrated near values of about 5 with a long tail extending beyond 100 (Figure 9.4b). Droplet radii in liquid water clouds show two populations, one near 7–10 μm over land and a second near 12–15 μm over oceans; however, there are some clouds that exhibit values greater than 20 μm that usually occur with very large optical thicknesses (Han et al., 1994). Liquid water path distributions grow progressively broader going from non-precipitating warm clouds, through non-precipitating cold clouds and precipitating warm clouds, to precipitating cold clouds (Lin and Rossow, 1996); but all distributions show some much larger values. Thus, a typical cloud can be defined by the most frequently occurring characteristics, but there are a significant number of clouds that have properties far from typical. These two different kinds of clouds, typical and atypical, can play different roles in the climate, as discussed later.

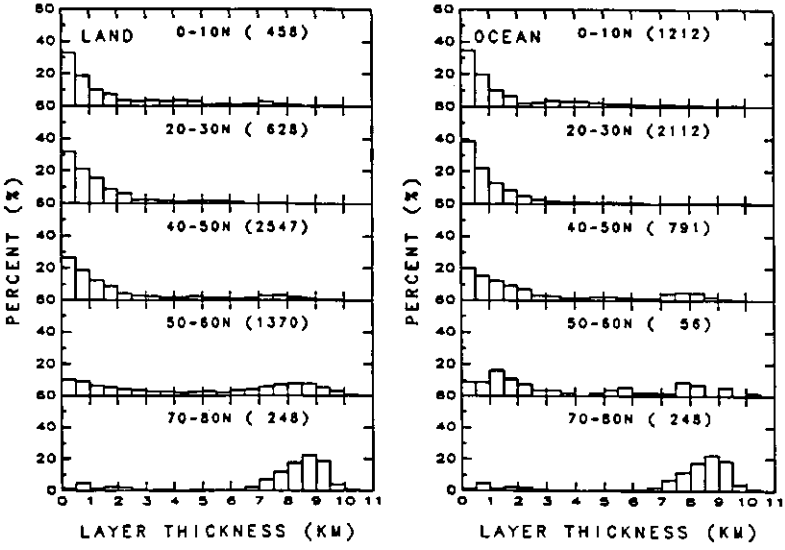

Figure 9.2: *Frequency distribution of cloud layer thicknesses for different latitude zones over land and ocean determined from rawinsonde humidity profiles (from Poore et al., 1995).*

The same cloud surveys can be used to describe the space and time scales over which clouds vary (Rossow and Cairns, 1995). Figure 9.5a shows the Fourier power spectrum of cloud-induced spatial variations of IR radiance as observed by satellites at three latitudes, while Figures 9.5b and 9.5c show the power spectrum of time variations at midlatitudes. The shapes of these spectra show that the largest variations occur at large space and time scales, of order $\sim$ 10,000 km and $\sim$ 10 days. The most notable exception is significant variations over a diurnal time scale, particularly at the larger spatial scale of a whole latitude zone (Figure 9.5b). The other important feature of cloud variations is that the space and time scales are coupled: very rapid variations occur primarily at the smaller spatial scales and planetary scale cloud features change significantly only over long time periods. Figure 9.6 shows that the Fourier power spectrum for tropical cloudiness becomes steeper (less variability at smaller scales) as the satellite observations are averaged over time; only for an average over 10 days is the power reduced at the largest spatial scales. There is little coherent spatial structure in the daily variability of cloud cover exhibited in an Empirical Orthogonal Function (EOF)

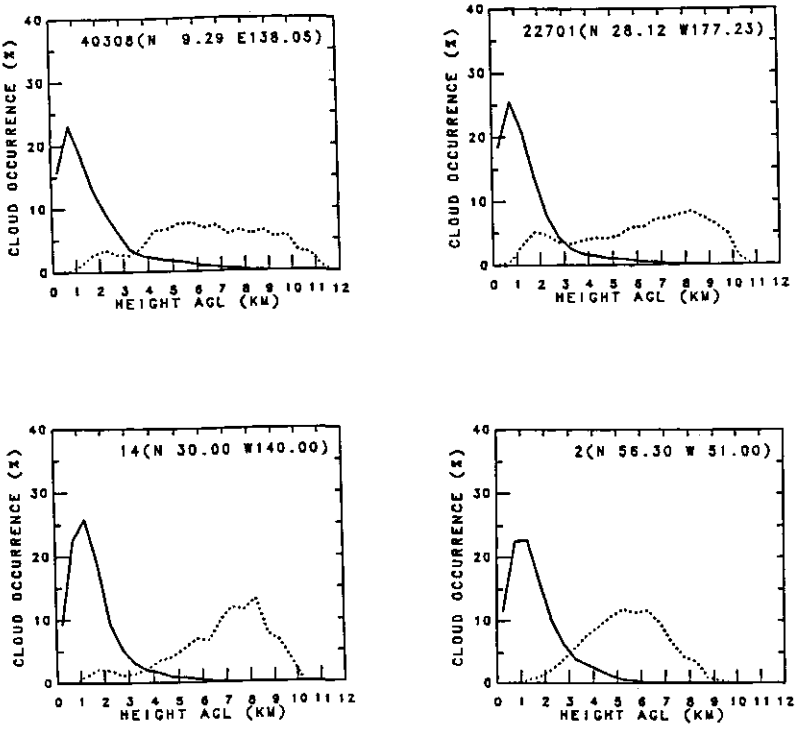

Figure 9.3: *Frequency of cloud layer occurrences in two-layer systems as a function of height for four ocean sites (latitude, longitude indicated) determined from rawinsonde humidity profiles (from Wang and Rossow, 1995).*

analysis for multi-month time periods. The first Principal Component (PC) exhibits a seasonal trend of tropical cloud cover in transition between wet and dry seasons; however, the spatial distribution of the other PCs is more noise-like at scales ≥ 500 km. The nearly even distribution of the variance over all of the eigenvectors (only the first one is significant) also shows that the daily variations have little coherent structure (except for diurnal variations which have been removed), although there is a hint of the subtropical jet streams in the optical thickness distributions. Thus, on time scales of ~ 30 days, there is little large scale structure in the cloud variations.

9.4 Global Patterns of Cloud Variations

There is much more coherent structure in the large scale patterns of cloud variation on longer time scales. This is shown by an EOF analysis performed on global monthly mean maps of cloud properties that eliminate the smaller scales of variation. Figure 9.7 shows the first four and only significant PCs and their eigenvectors (EV) for cloud cover (similar results obtain for cloud optical thickness and top pressure). The first notable feature of the cloud cover variation is that the largest changes occur only with location: more than 70% of the variation is contained

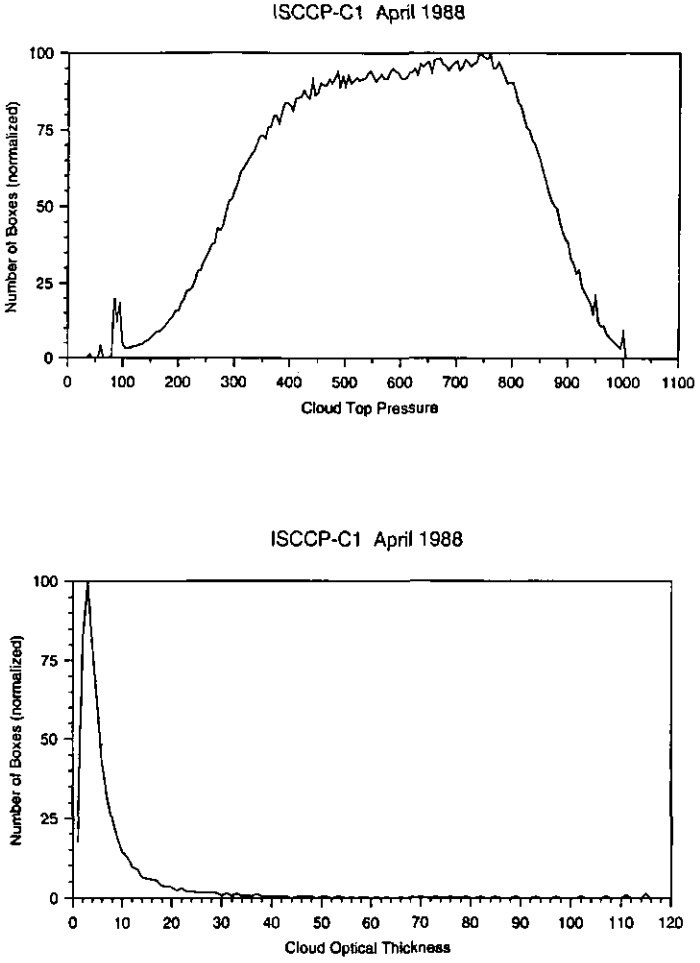

Figure 9.4: *Frequency distributions of (a) cloud top pressure and (b) visible optical thickness observed from satellites (from Rossow and Cairns, 1995).*

in the first PC which is essentially constant with time (Rossow et al., 1993; Rossow and Cairns, 1995). For cloud optical thickness and top pressure the first PC explains 60–65% of the total variability. The characteristic global pattern of this geographic variability marks the classical climate regimes produced by the large scale atmospheric circulation.

At lower latitudes, regimes dominated by mean upward motions and intense convective activity are associated with large cloud cover (positive contours in the first PC), low optical thicknesses and water contents, and a predominance of high level and low level cloudiness. Embedded in these regions is the highest concentration of dense precipitating systems. The low latitude regimes over oceans, dominated by mean downward motions with convection confined to the boundary layer, are associated with two types of low-level cloud regimes: one with very small

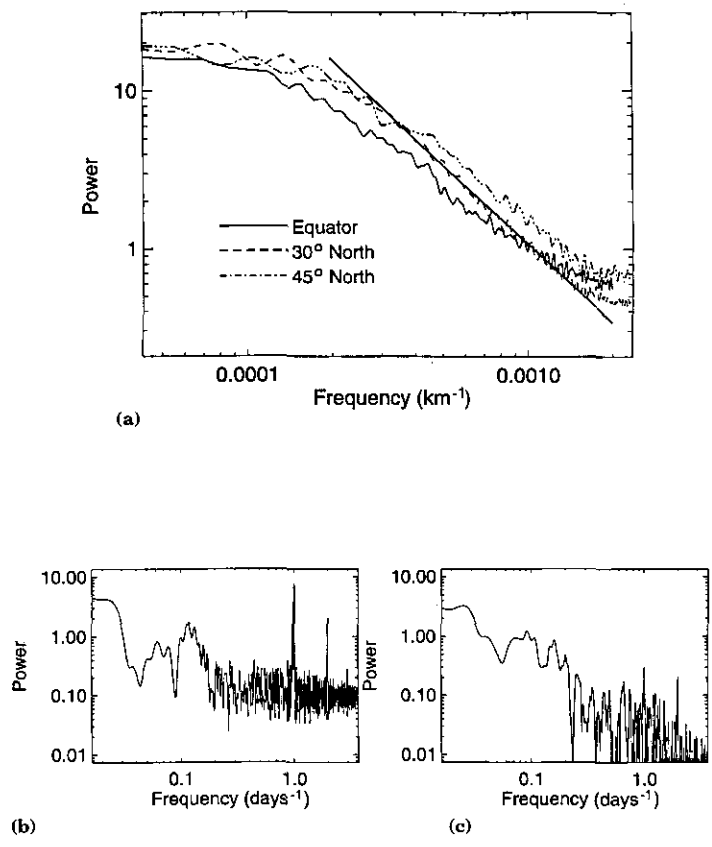

Figure 9.5: *Fourier power spectra of the (a) space and (b,c) time variations of cloudiness (from Rossow and Cairns, 1995). Analysis for spatial variations is performed at the equator (solid line), at 30° N (dashed line) and at 45° N (dot-dash line). A line representing a (-2)-power law is shown for reference. The time variations are analyzed for a whole latitude zone (b, 45° N) and for one location (c, Europe) in the same zone.*

cloud cover and optical thicknesses and one with very large cloud cover and moderate optical thicknesses. Over land, deserts, the downward motion regime exhibits very low cloud cover and optical thickness and a predominance of high-level cloudiness. Midlatitudes, where large scale cyclonic storms dominate the general circulation over oceans, are characterized by large cloud cover, large optical thicknesses, cloud tops in the middle troposphere and cloud bases near the surface. Although the frequency of dense precipitating clouds is less at midlatitudes, the area-average cloud optical thicknesses are larger than in the tropics. Polar regions present a more complicated and poorly measured situation ranging from fairly dense, low-level cloudiness in summertime to fairly tenuous, middle and high level cloudiness in wintertime (e.g., Curry and Ebert, 1992).

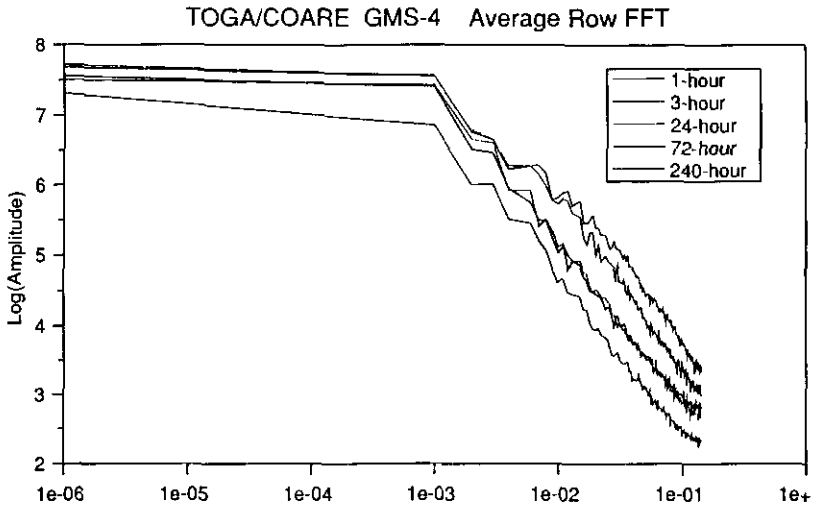

Figure 9.6: *Fourier power spectra of space variations in infrared satellite images of the western equatorial Pacific (the TOGA-COARE region), progressing downward from a single image to images averaged over the indicated time intervals (from Rossow and Cairns, 1995).*

The second notable feature of the cloud cover variation is that the largest time variation is the annual cycle (second and third PC in Figure 9.7) which is dramatically different at lower, middle, and higher latitudes (Rossow et al., 1993). The largest annual variations in cloud properties occur in the tropics with the seasonal shifts of the Inter Tropical Convergence Zone (ITCZ), although polar cloudiness may undergo relatively large seasonal variations in cloud water content. The tropical annual cycle exhibits increases in cloud cover, optical thickness, and cloud top height from wintertime (dry season) to summertime (wet season). In midlatitudes, the magnitude of the annual cycle is much smaller, particularly over oceans, and exhibits decreases in cloud cover, optical thickness and cloud top height from wintertime (cold season) to summertime (warm season). In some land areas, however, the summertime cloud top heights and cloud cover might be slightly larger than wintertime values. Polar region cloudiness may not exhibit much seasonal variation in cloud cover, but current poor observations suggest some changes in cloud heights and optical thicknesses may occur (Curry and Ebert, 1992).

The fact that the annual cycle is represented by two PCs, one with a phase coinciding with the solstices and one with the equinoxes, indicates that the amplitude and phase of the annual cycle vary with location, so that the description given above is only an approximation for a much more complicated variation. Significant differences between the hemispheres appear in the vicinity of the Asian monsoons, which are more extensive in boreal summer than in austral summer, in the eastern Pacific ITCZ, which remains in the northern hemisphere year round, over Brazil, which exhibits much more cloudiness in summer than winter, and over the two eastern Pacific marine stratus regions, which vary in phase over the year in both hemispheres. Although the southern hemisphere exhibits much less annual variation in temperature than the northern hemisphere, it exhibits much more annual variation in total cloud amount.

The third notable feature of the cloud variations shown in Figure 9.7 is that variations on time scales longer than one year are very small: the fourth PC (2% of the variation) includes

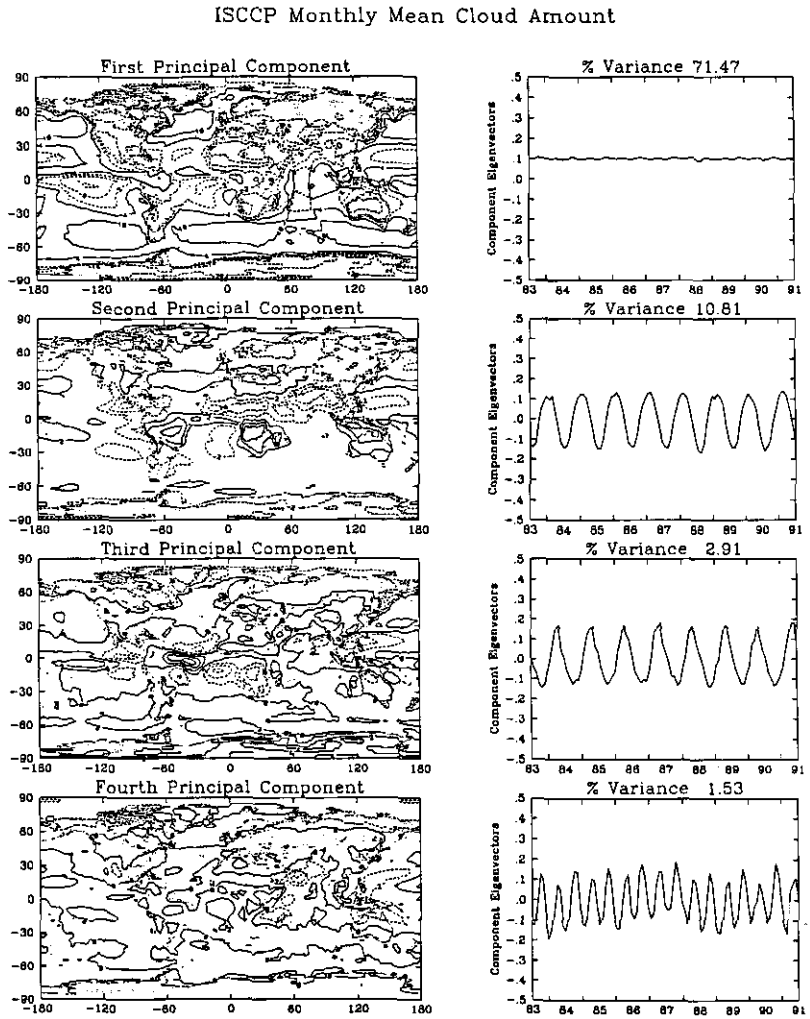

Figure 9.7: *Empirical Orthogonal Function analysis of monthly mean, total cloud cover variations from ISCCP over the whole globe for eight years (1983-1991) (from Rossow and Cairns, 1995).*

a semi-annual variation and a slow variation over the whole data record. Thus, despite the common impression that clouds vary a lot, most of this variation is confined to time scales less than one month; on longer time scales the cloudiness of Earth is remarkably constant (Rossow et al., 1993; Rossow and Cairns, 1995). However, this does not mean that small, but systematic variations of cloud do not occur and that they are not important. Rather, given the estimated sensitivity of the climate to small changes in the radiative balance (e.g. Hansen et al., 1984), even cloud changes of a few percent can be important. Figure 9.8 illustrates one of the better

known systematic changes in cloudiness that occurs on a time scale of 3–10 years, namely the El Niño-Southern Oscillation (ENSO) events. The figure shows the EV for global high-level cloudiness, with the mean annual cycle removed, from two satellite datasets (NIMBUS-7: Stowe et al., 1988; ISCCP) compared with the variations from the mean of tropical sea level pressure differences. This figure shows that, while there is some similarity in the changes associated with these two ENSO events, there are also large differences in detail, so that a proper characterization of the average ENSO variations requires a long enough data record to sample many (at least 3–10) such events. The currently available datasets cover only about four events.

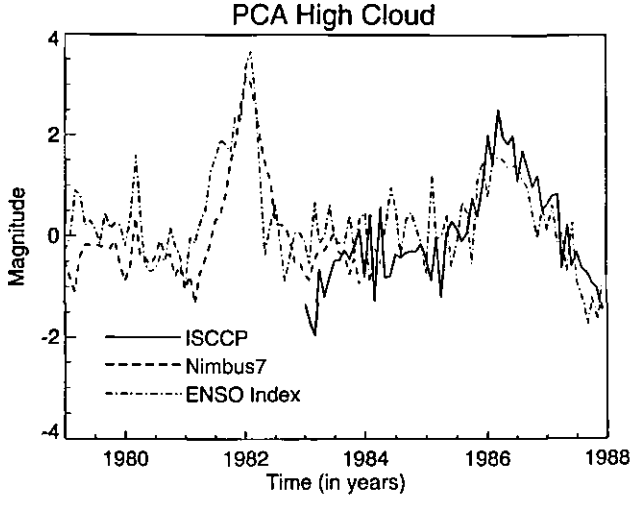

Figure 9.8: *Empirical Orthogonal Function analysis of the NIMBUS-7 and ISCCP high-level cloud amounts compared with the ENSO index for the El Niños in 1982–83 and 1986–87 (from Rossow and Cairns, 1995).*

The one systematic variation of clouds at time scales less than one month is the diurnal cycle (Figure 9.5b). Figure 9.9 illustrates some of the variety of cloud diurnal cycles exhibited in different climate regimes (Carlson et al., 1996). In general the diurnal variation amplitudes are largest at low latitudes. A notable feature is that the phase of the diurnal cycle of low-level cloudiness over oceans is very different than over land (not shown). Low-level clouds over land increase to maximum cover and height in early afternoon, coincident with or slightly later than the maximum surface temperatures resulting from the peak solar heating of the day, whereas low-level clouds over ocean increase to maximum cover and height near or just before dawn, even though maximum surface temperatures still occur in early afternoon. The other notable feature is that the diurnal variations of middle and high-level clouds over both ocean and land have a different phase than that of low-level clouds and that the diurnal variation of high-level clouds over land varies significantly with season, being largest in local summertime (Figure 9.9).

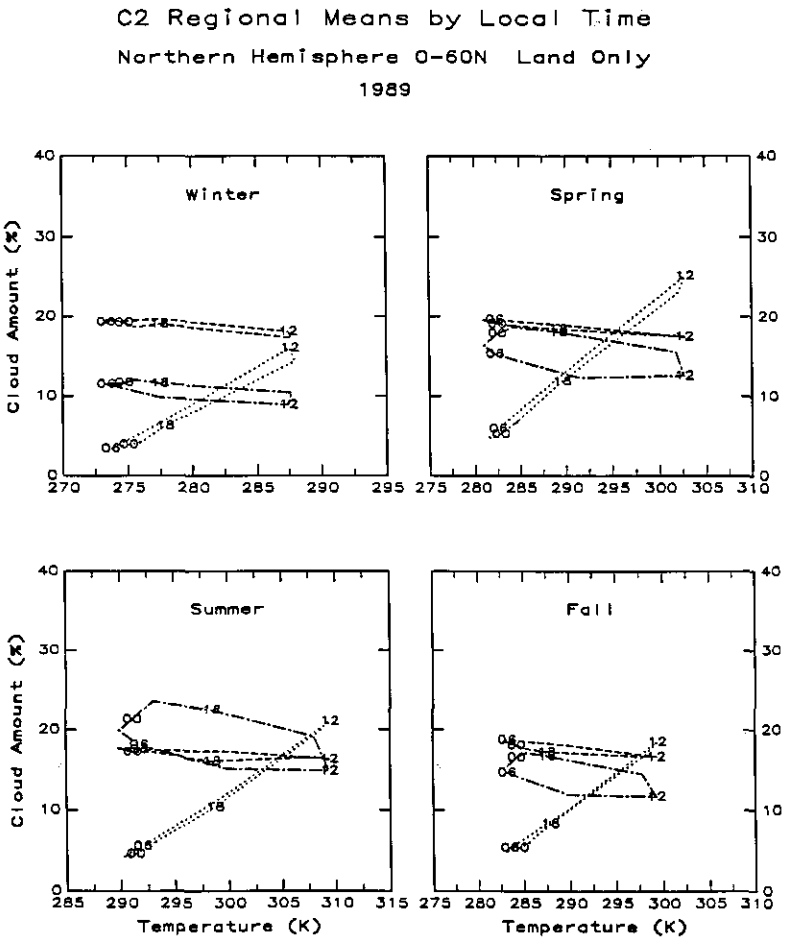

Figure 9.9: *Diurnal phase diagrams of cloudiness for different climate regimes.*

9.5 Classification of Clouds

Clouds are classified in surface observations on the basis of the estimated height of their bases above the local surface topography and on their shape (e.g. Warren et al., 1986). While cloud base heights of low-level clouds can be estimated with good accuracy, the discrimination between middle and high clouds may depend more on morphology (cf. Wang and Rossow, 1995). There are three main height classes: low (0–2 km), middle (2–4 km at higher latitudes and 2–6 km at lower latitudes), and high. There are three main cloud types or shapes: cumuloform, stratoform and cirroform. Cumuloform clouds form under the influence of small scale convective turbulence, whereas stratoform clouds are associated with larger scale synoptic motions. Cirroform clouds are indicative of a change of phase from liquid to ice. Different cloud types are associated with different kinds of weather: most notably fair weather is associated

with frequent occurrence of cumulus clouds (low-level cumuloform) and/or cirrus (high-level cirroform) clouds, whereas foul weather clouds producing precipitation are associated with cumulonimbus (vertically extensive cumuloform) clouds and nimbostratus (vertically extensive and thick stratoform) clouds. Figure 9.10 compares the zonal average amounts of cirrus and cumulus as determined from both surface and satellite observations. Both these types of clouds have relatively uniform latitudinal distributions. Cumulonimbus and nimbostratus clouds, together with all high clouds, have noticeable concentrations in the tropics and midlatitudes, respectively, associated with the regions that have the most frequent and active storms in our atmosphere. These locations are also associated with higher total cloud amounts (Figure 9.7).

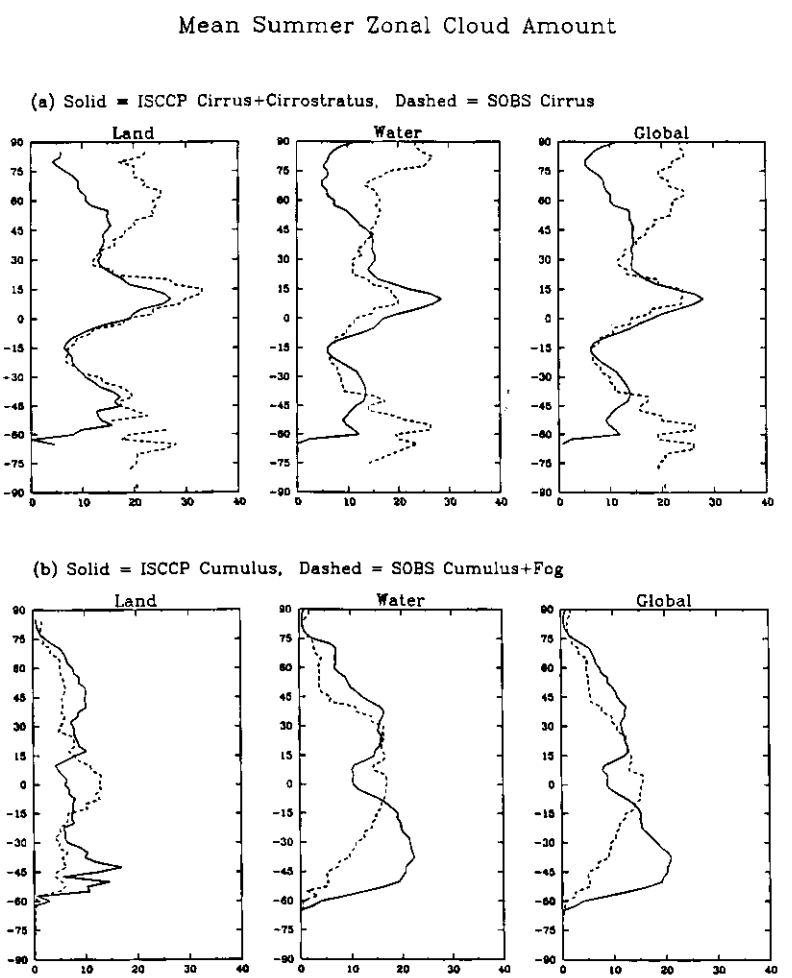

Figure 9.10: *Zonal, seasonal mean (a) cirrus and (b) cumulus cloud amounts from surface weather observations (SOBS - dashed lines) and from satellite (ISCCP - solid lines).*

Clouds are classified in satellite observations by the location of their tops and their optical thicknesses (Rossow and Schiffer, 1991; see also Liu et al., 1995). Three height classes are defined by cloud top pressures (equivalent to height above mean sea level): low-level clouds have top pressures > 680 hPa (height 3 km), middle clouds have top pressures < 680 hPa and > 440 hPa (height 6 km), and high clouds have top pressures < 440 hPa. The optical thickness categories are more complicated as shown in Figure 9.11. The distributions of cloud properties in three different climate regimes are shown in Figure 9.12. We note that in the subtropical

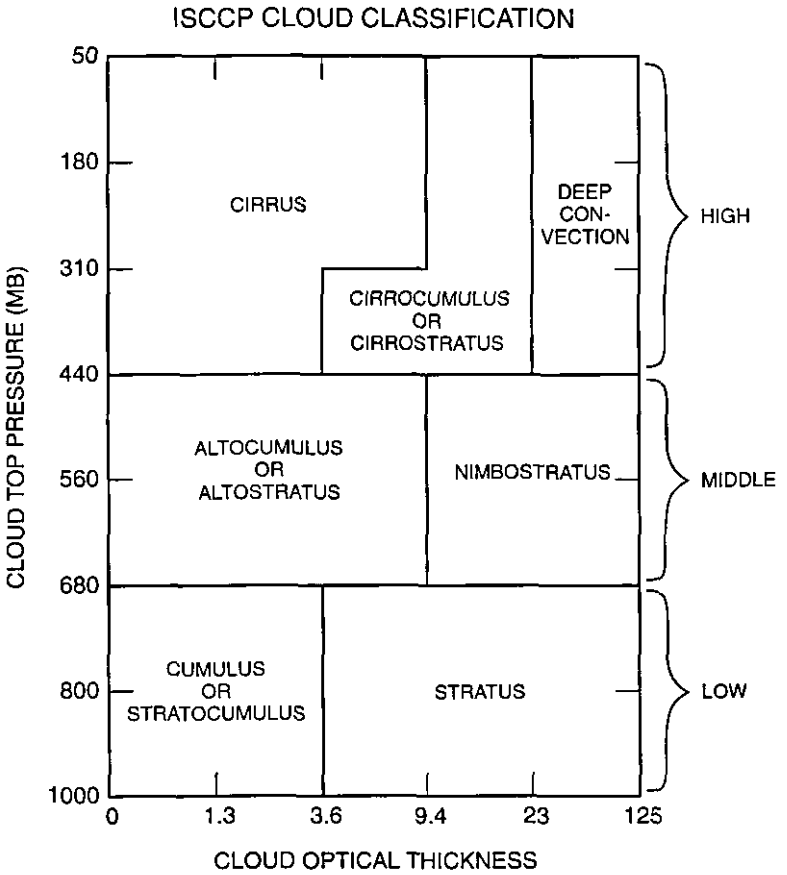

Figure 9.11: *Cloud classification scheme using satellite-determined cloud top pressures and optical thicknesses (from Rossow and Schiffer, 1991). Cloud type names are meant to be qualitative only.*

regimes the most frequent type is low-level optically thin clouds. In midlatitudes there is a mixture of low and high-level optically thin and middle-to-high level and optically thick clouds. In the tropics, in addition to a shift of the optically thicker clouds to a much higher level, a third type of cloud is apparent with moderately high tops and moderate optical thicknesses.

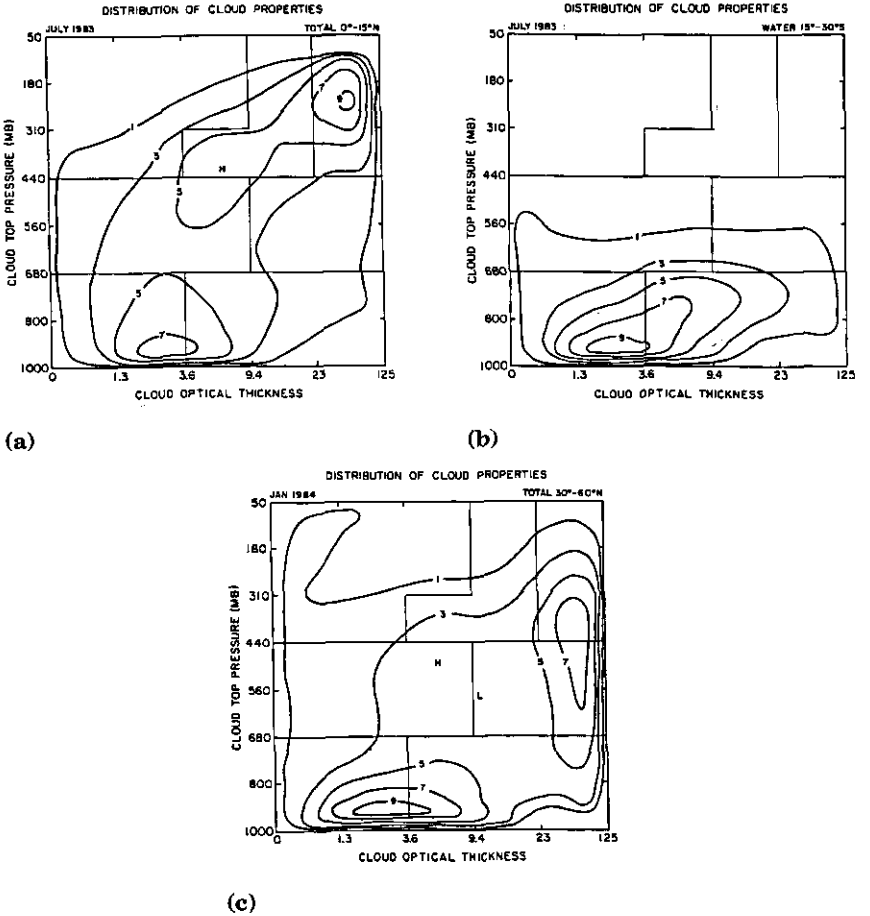

Figure 9.12: *Frequency distributions of clouds classified in satellite observations for (a) the tropics, (b) the subtropical oceans and (c) midlatitude land areas.*

The latter is identified as the stratoform anvil cloud in large convective complexes (Machado and Rossow, 1993).

Satellite measurements of microwave wavelength radiation can indicate the presence of rainfall and the combination of microwave and visible/infrared measurements can be used to estimate the approximate mixture of ice and liquid water (Lin and Rossow, 1994; 1996), as shown in Figure 9.13.

Coincident observations indicate a close link between the amounts of ice and liquid water in the clouds and the presence of rainfall: rainfall is much more likely in clouds with optical thicknesses ≥ 60 (equivalent to water path values ≥ 40 mg/cm^2), but even more likely if cloud tops are high enough that significant ice is present (cf., Liu et al., 1995). Hence, we identify the cloud in the upper right hand corner of Figure 9.12 to be associated with precipitation produced in storms. Plotting the geographic distribution of these cloud types (Figure 9.14) shows a

striking resemblance to the distribution determined by surface observers. The similarity of the distributions observed from surface and satellite of cirrus and cumulus cloud amounts and cumulonimbus and nimbostratus suggests a primary link between the weather producing clouds and their observed radiative properties.

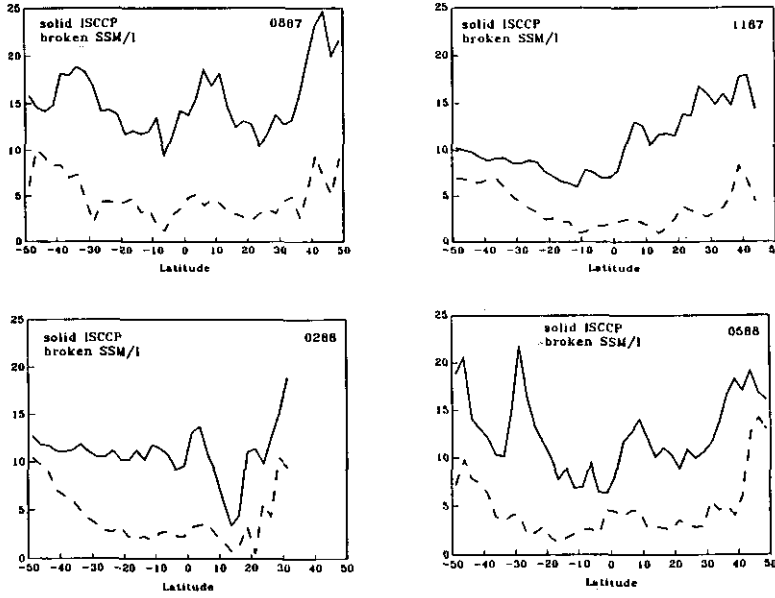

Figure 9.13: *Zonal, monthly mean liquid (dashed line) and total (solid line) water path for non-precipitating clouds in four seasonal months: the difference between total and liquid water path is approximately the ice water path (from Lin and Rossow, 1996).*

9.6 Cloud Systems

Comparison of the large scale pattern of the geographic distribution of cloud properties to some attributes of the mean atmospheric circulation shows that the main dynamic process that controls cloudiness in the atmosphere is vertical motions in the general atmospheric circulation. This association of clouds and vertical motions has long been studied at much smaller scales (Cotton and Anthes, 1989). Although the mean vertical motion pattern resembles the mean pattern of cloud properties, it is the vertical motions in individual storm systems that determine the largest values of cloud water content and top height. The shapes of the cloud property distributions suggest a two-population model: one large background population composed of optically thinner clouds with small vertical extents and one relatively sparse population composed of optically thicker clouds with much larger vertical extents. Averaging the observations produces values more similar to the more frequent (more typical) clouds in the background population. The background population dominates the radiation balance (Rossow and Zhang, 1995), but the smaller storm population produces the precipitation (Lin and Rossow, 1996). The object of further research is to determine what atmospheric conditions produce these two cloud populations and what relation exists between them.

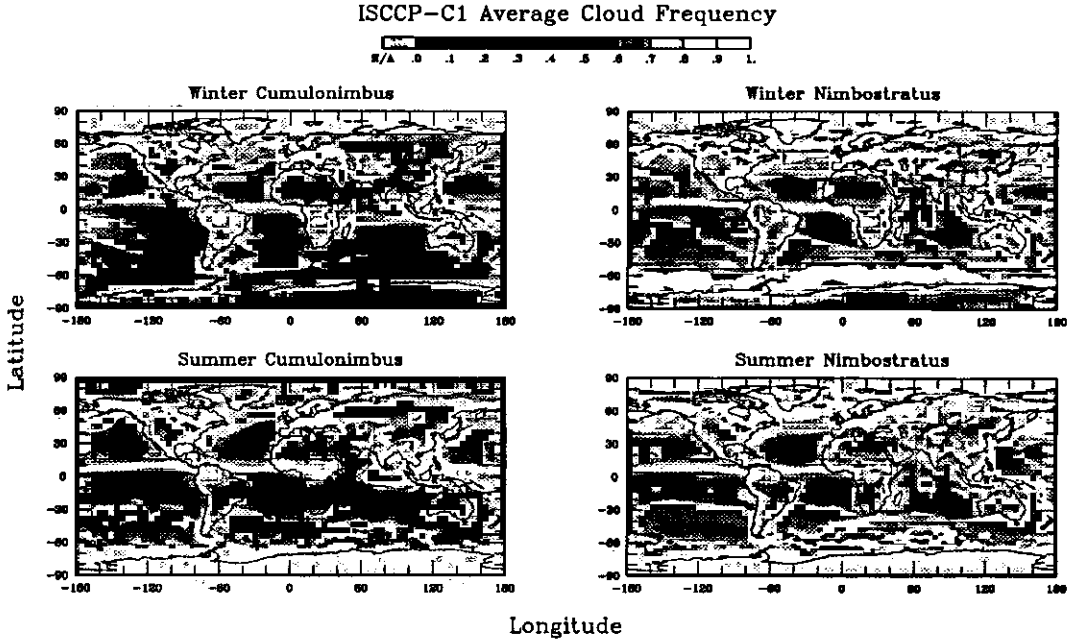

Figure 9.14: *Geographic distributions of seasonal mean frequencies of occurrence of cumulonimbus and nimbostratus (see Figure 9.11) from the ISCCP satellite dataset.*

What atmospheric conditions produce deep convection in the tropics and what kinds of clouds are produced? The simplest answer to the first question is that surface heating by sunlight produces buoyant parcels of moisture-laden air near the surface that, once condensation begins, can rise all the way to the tropopause. This simple model predicts a concentration of convection over regions with high surface temperatures; but the actual distribution of such convective systems contradicts this simple prediction in several ways. The hottest surface temperatures appear in North Africa and other nearly cloud-free deserts where there is no convection. The hottest ocean water is in the western Pacific and eastern Indian ocean, yet only the former is persistently covered by convection. A closer look at the western Pacific shows that convection does not occur everywhere, suggesting other factors that influence the occurrence of convection (Figure 9.15). Combining satellite observations of cloud properties with surface weather observations shows that it is the large scale circulation and its influence on the boundary layer humidity that sometimes inhibits convection over warm oceans and that the ocean temperature is important for triggering convection because the tropical atmosphere is more nearly isothermal than the ocean surface (Fu et al., 1990, 1994).

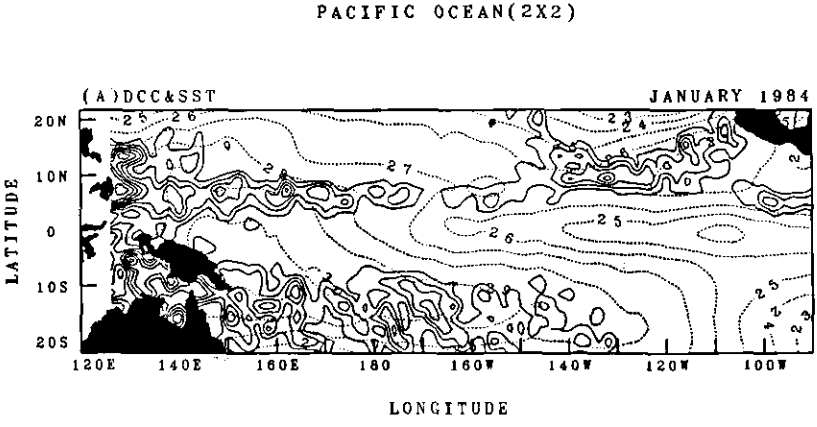

Figure 9.15: *Average distribution of sea surface temperature in °C (dashed contours) and frequency of occurrence of deep convective cloudiness (solid contours) for January 1984 over the tropical Pacific (from Fu et al., 1994).*

The first survey of the cloud properties associated with deep convection shows two notable features: strong concentration of convection over land (but not the hottest land areas) and the strong variations of cloud properties with the size of the system (Machado and Rossow, 1993). There is a particularly suggestive pattern to the size dependence: as the system size grows, so does the area covered by convective towers. As they grow larger in horizontal dimension, they extend higher into the atmosphere (lower cloud top temperatures in Figure 9.16). Surface and aircraft observations have also correlated the size and vertical extent of convective towers with the strength of the updrafts (e.g. Betts, 1973; Zipser and LeMone, 1980). The main change in the stratoform cloud component of these systems as their size increases is that their optical thicknesses or albedos increase (Figure 9.16). Since these stratoform clouds tend to have nearly constant base and top locations (e.g., Gamache and Houze, 1982; Tollerud and Esbensen, 1985), the albedo increase is equivalent to a water content increase, suggesting that precipitation also becomes more frequent (Lin and Rossow, 1996).

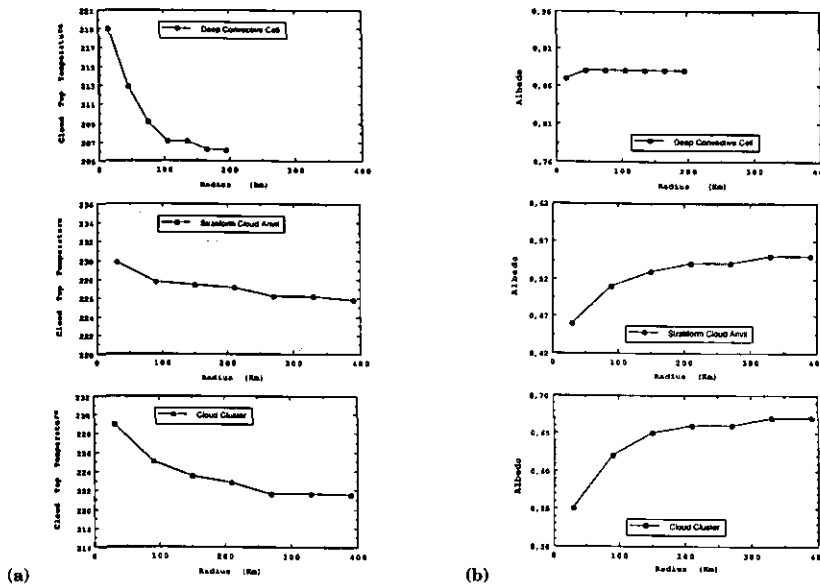

Figure 9.16: *Variation of average (a) cloud top temperature and (b) cloud visible albedo with the radius of tropical convective complexes for the convective towers (upper panel), the stratoform anvil clouds (middle panel) and the whole cloud cluster (lower panel) from satellite observations (from Machado and Rossow, 1993).*

What kinds of clouds are produced by midlatitude cyclones? This type of investigation is only just beginning. Early results correlating cloud types determined from satellite data with meteorological information on winds and temperatures (Lau and Crane, 1995) show that the optically thicker and generally higher clouds occur in association with midlatitude cyclones, particularly in those parts of these systems where vertical motions are strongest (Figure 9.17). Moreover, the high-topped and optically thicker clouds concentrate in the warm sector where rising motions predominate, while the thin cirrus clouds congregate in the cold sector where sinking motions predominate (Figure 9.18). These early results encourage studies to determine quantitative relationships between the strength of these storm systems and the properties of the clouds they produce. Two kinds of non-storm clouds are receiving a lot of attention: cirrus clouds far from either convective complexes or cyclones (e.g. Sassen et al., 1989) and marine boundary layer cloudiness in the subtropics, primarily in the higher cloud cover regimes (e.g. Betts and Boers, 1990). Since this research is in its early stages, explanations connecting the larger scale atmospheric motions to the properties of these clouds are not available as yet.

9.7 Future Studies

The last few studies described above point the way to research that has just begun and has the potential to determine how atmospheric motions affect cloud properties and precipitation. By combining the satellite and surface cloud measurements with observations of atmospheric conditions (temperature, humidity, winds) for many individual storms, the relationships between

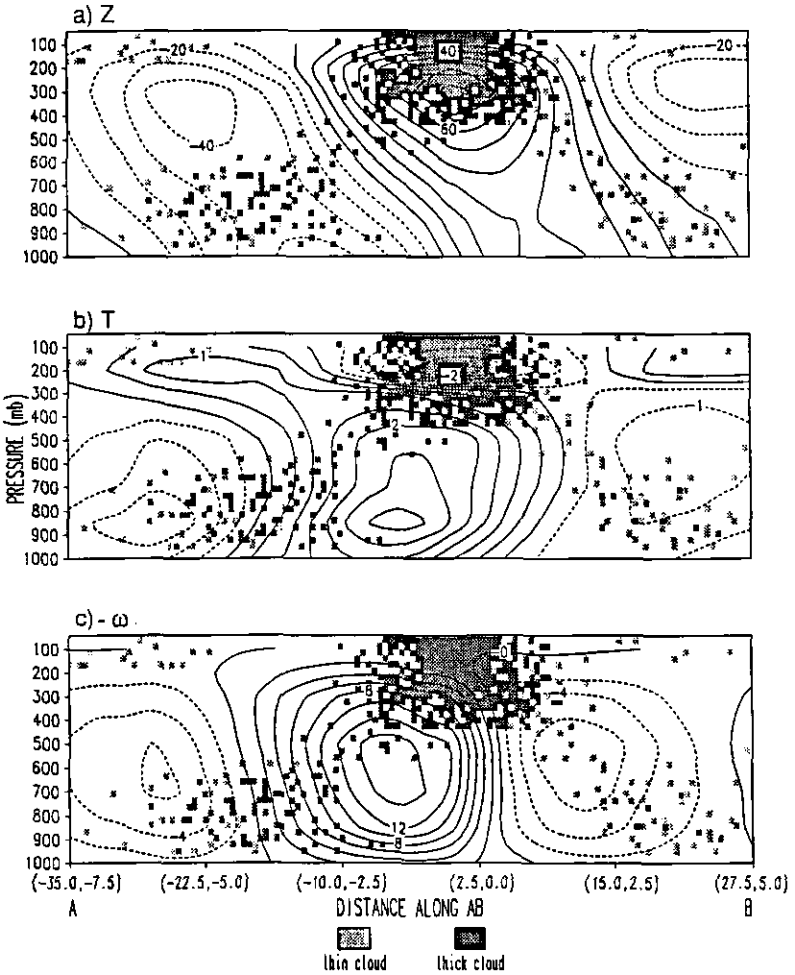

Figure 9.17: *Composite distribution of clouds with different optical thicknesses, indicated by the shading in small squares, as function of top pressure and position along the motion track of midlatitude cyclones compared with the distribution of anomalies in geopotential height (Z), temperature (T), and vertical motion (ω) (from Lau and Crane, 1995).*

the strength of these storms and the cloud properties may be discerned. Similarly conditions in fair weather may linked to the properties of boundary layer and cirrus clouds. The satellite cloud properties can be used to determine their effects on the radiation balance (e.g. Rossow and Zhang, 1995). Other satellite measurements can be combined to determine the relation of cloud properties and precipitation (e.g. Lin and Rossow, 1996). For the first time, we have global, multi-year collections of all of these quantities organized together that would allow this type of study to be conducted. However, a key missing element is the capability to determine these cloud properties at the same time at scales 5 km and 30 min, as would be possible if

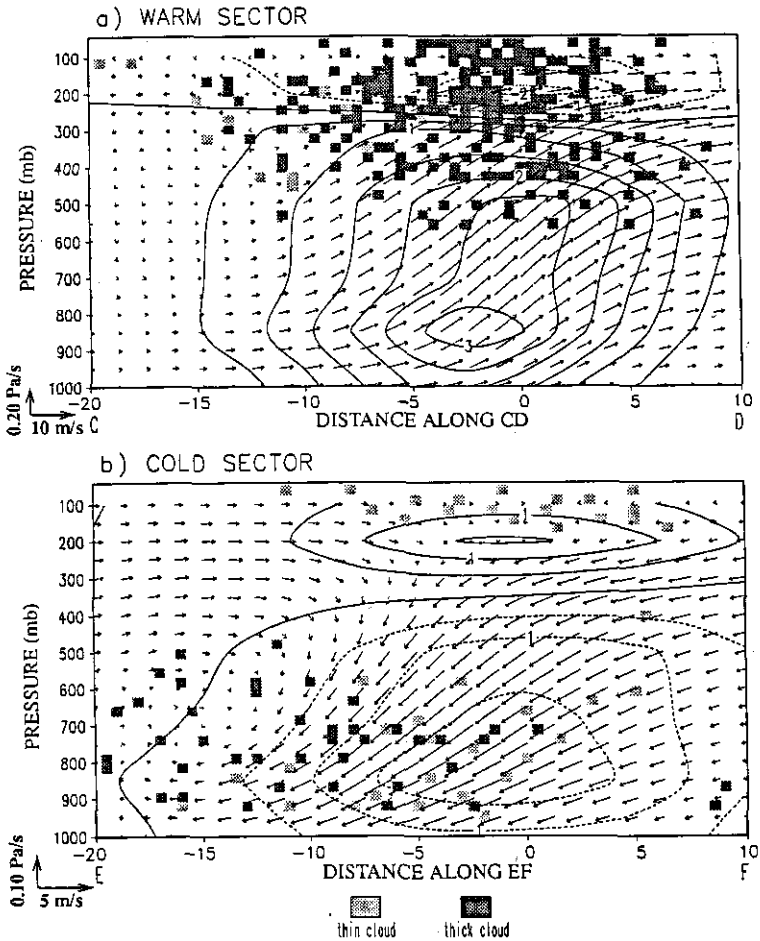

Figure 9.18: *Composite distribution of clouds with different optical thicknesses, indicated by the shading in small squares, as function of top pressure and across the motion track of midlatitude cyclones compared with the distribution of anomalies in temperature (contours) and winds (arrows) in the (a) warm sector and (b) cold sector of the cyclone (from Lau and Crane, 1995).*

several instruments were on a single spacecraft in geostationary orbit. Such a cloud-physics satellite mission would still have to include a cloud profiling radar to determine cloud vertical structures. Such a mission would also be valuable in lower orbit where measurements would be limited to larger scales.

For more information, see the ISCCP Web Home Page at URL = http://isccp.giss.Nasa.gov

9.8 References

Betts AK, Boers R (1990) A cloudiness transition in a marine boundary layer. *J Atmos Sci* 47: 1480–1497

Carlson BE, Lacis AA, Rossow WB (1993) Tropospheric gas composition and cloud structure of the Jovian North Equatorial Belt. *J Geophys Res* 98: 5251–5290

Carlson BE, Cairns B, Rossow WB (1996) Spatial and temporal characterization of diurnal cloud variability using ISCCP. *J Climate*, in press

Curry JA, Ebert EE (1992) Annual cycle of radiation fluxes over the Arctic Ocean: Sensitivity to cloud optical properties. *J Climate* 5: 1267–1280

Fu R, Del Genio AD, Rossow WB (1990) Behavior of deep convective clouds in the tropical Pacific deduced from ISCCP radiance data. *J Climate* 3: 1129–1152

Fu R, Del Genio AD, Rossow WB (1994) Influence of ocean surface conditions on atmospheric vertical thermodynamic structure and deep convection. *J Climate* 7: 1092–1108

Gamache JF, Houze RA (1982) Mesoscale air motions associated with a tropical squall line. *Mon Wea Rev* 110: 118–135

Goody RM, Yung YL (1989) *Atmospheric Radiation, Theoretical Basis.* Oxford, New York, 519 pp

Greenwald TJ, Stephens GL, Vonder Haar TH, Jackson DL (1993) A physical retrieval of cloud liquid water over global oceans using Special Sensor Microwave/Image (SSM/I) observations. *J Geophys Res* 98: 18.471–18.488

Hahn CJ, Warren SG, London J (1995) The effect of moonlight on observation of cloud cover at night and application to cloud climatology. *J Climate* 8: 1429–1446

Han Q-Y, Rossow WB, Lacis AA (1994) Nearglobal survey of effective cloud droplet radii in liquid water clouds using ISCCP data. *J Climate* 7: 465–497

Hansen JE, Travis LD (1979) Light scattering in planetary atmospheres. *Space Sci Rev* 16: 527–610

Hansen J, Lacis A, Rind D, Russell G, Stone P, Fung I, Ruedy R, Lerner J (1984) Climate sensitivity: analysis of feedback mechanisms. Climate Processes and Climate Sensitivity, *Geophys. Monogr. Ser.* Vol. 29, AGU. J.E. Hansen and T. Takahashi (eds.), Washington, D.C., 130–163

Kent GS, Winker DM, Osborn MT, Skeens KM (1993) A model for the separation of cloud and aerosol in SAGE II occultation data. *J Geophys Res* 98: 20.725–20.735

Kropfli RA, Matsarov SY, Uttal T, Oss BW, Frisch AS, Clark KA, Partran BW, Snider JB (1995) Studies of cloud microphysics with millimeter radar. *Atmos Res* 35: 299–313

Lau N-C, Crane MW (1995) A satellite view of the synoptic-scale organization of clouds in midlatitude and tropical circulation systems. *Mon Wea Rev* 123: 1984–2006

Liao X, Rossow WB, Rind D (1995) Comparison between SAGE II and ISCCP high-level clouds, Part I: Global and zonal mean cloud amounts. *J Geophys Res* 100: 1121–1135

Liao X, Rossow WB, Rind D (1995) Comparison between SAGE II and ISCCP high-level clouds, Part II: Locating cloud tops. *J Geophys Res* 100: 1137–1147

Lin B, Rossow WB (1994) Observations of cloud liquid water path over oceans: Optical and microwave remote sensing methods. *J Geophys Res* 99: 20.907–20.927

Lin B, Rossow WB (1996) Cloud water path observations over oceans using ISCCP and SSM/I data. *J Climate,* in press

Liu G, Curry JA (1992) Retrieval of precipitation from satellite microwave measurements using both emission and scattering. *J Geophys Res* 97: 9959–9974

Liu G, Curry JA (1992) Determination of characteristic features of cloud liquid water from satellite microwave measurements. *J Geophys Res* 98: 5069–5092

Liu G, Curry JA, Sheu R-S (1995) Classification of clouds over the western equatorial Pacific Ocean using combined infrared and microwave satellite data. *J Geophys Res* 100: 13.811–13.826

Poore K, Wang J-H, Rossow WB (1995) Cloud layer thicknesses from a combination of surface and upper air observations. *J Climate* 8: 550–568

Rossow WB, Garder LC, Lacis AA (1989) Global, seasonal cloud variations from satellite radiance measurements. Part I: Sensitivity of analysis. *J Climate* 2: 419–462

Rossow WB, Schiffer RA (1991) ISCCP cloud data products. *Bull Amer Meteor Soc* 72: 2–20

Rossow WB, Walker AW, Garder LC (1993) Comparison of ISCCP and other cloud amounts. *J Climate* 6: 2394–2418

Rossow WB, Cairns B (1995) Monitoring changes of clouds. *Climatic Change,* 31: 305–341

Rossow WB, Zhang Y-C (1995) Calculation of surface and topofatmosphere radiative fluxes from physical quantities based on ISCCP datasets, Part II: Validation and first results. *J Geophys Res* 100: 1167–1197

Sassen K, Starr DO, Uttal T (1989) Mesoscale and microscale structure of cirrus clouds: Three case studies. *J Atmos Sci* 46: 371–396

Schiffer RA, Rossow WB (1983) The International Satellite Cloud Climatology Project (ISCCP): The first project of the World Climate Research Programme. *Bull Amer Meteor Soc* 64: 779–784

Stephens GL (1994) *Remote Sensing of the Lower Atmosphere. An Introduction.* Oxford, New York, 523 pp

Stowe LL, Wellemeyer CG, Eck TF, Yeh HYM and the NIMBUS-7 Cloud Data Processing Team (1988) NIMBUS-7 global cloud climatology. Part I: Algorithms and validation. *J Climate* 1: 445–470

Tollerud EI, Esbensen SK (1985) A composite life cycle of nonsquall mesoscale convective systems over the tropical ocean. Part I: Kinematic fields. *J Atmos Sci* 42: 823–837

Wang J, Rossow WB (1995) Determination of cloud vertical structure from upper air observations. *J Appl Meteor* 34: 2243–2258

Wang P-H, McCormick MP, Minnis P, Kent GS, Yue GK, Skeens KM (1995) A method for estimating vertical distribution of the SAGE II opaque cloud frequency. *Geophys Res Lett* 22: 243–246

Warren SG, Hahn CJ, London J, Chervin RM, Jenne RL (1986) Global distribution of total cloud and cloud type amounts over land. 29 pp. + 200 maps, (NTIS number DE87-00-6903)

Warren SG, Hahn CJ, London J, Chervin RM, Jenne RL (1988) Global distribution of total cloud and cloud type amounts over the ocean. 42 pp. + 170 maps, (NTIS number DE90-00-3187)

Woodbury GE, McCormick MP (1986) Zonal and geographical distribution of cirrus clouds determined from SAGE II data. *J Geophys Res* 91: 2775–2785

Wylie DP, Menzel WP (1989) Two years of cloud cover statistics using VAS. *J Climate* 2: 380–392

Wylie DP, Menzel WP, Woolf HM, Strabala KI (1994) Four years of global cirrus cloud statistics using HIRS. *J Climate* 7: 1972–1986

Zhang Y-C, Rossow WB Lacis AA (1995) Calculation of surface and topofatmosphere radiative fluxes from physical quantities based on ISCCP datasets, Part I: Method and sensitivity to input data uncertainties. *J Geophys Res* 100: 1149–1165

Zipser EJ, LeMone MA (1980) Cumulonimbus vertical velocity events in GATE. Part II: Synthesis and model core structure. *J Atmos Sci* 37: 2458–2469

General Reading

Cotton WR, Anthes RA (1989) *Storm and Cloud Dynamics.* Academic, San Diego, 880 pp

Goody RM, Yung YL (1989) *Atmospheric Radiation, Theoretical Basis.* Oxford, New York, 519 pp

Houze RA (1993) *Cloud Dynamics.* Academic, San Diego, 573 pp

Ludlam FH (1980) *Clouds and Storms.* Pennsylvania State University Press, University Park, 405 pp

Stephens GL (1994) *Remote Sensing of the Lower Atmosphere, An Introduction.* Oxford, New York, 523 pp